Strong Atmospheric New Particle Formation in Winter, Urban Shanghai, China

Shan XIAO[1,2], Mingyi WANG[1,2], Lei YAO[1,2], Markku KULMALA[3], Bin ZHOU[1,2], Xin YANG[1,2], Jianmin CHEN[1,2], Dongfang WANG[4], Qingyan FU[4], Douglas R. WORSNOP[5], Lin WANG[1,2*]

[1]*Shanghai Key Laboratory of Atmospheric Particle Pollution and Prevention (LAP[3]), Department of Environmental Science & Engineering, Fudan University, Shanghai 200433, P. R. China*

[2]*Fudan Tyndall Centre, Fudan University, Shanghai 200433, P. R. China*

[3]*Department of Physics, University of Helsinki, 00014 Helsinki, Finland*

[4]*Shanghai Environmental Monitoring Centre, Shanghai 200030, P.R. China*

[5]*Aerodyne Research, Billerica, MA 01821, USA*

**Corresponding author: tel,+86-21-65643568; fax, +86-21-65642080, email, lin_wang@fudan.edu.cn*

Abstract Particle size distributions in the range of 1.34-615 nm were recorded from Nov. 25th, 2013 to Jan. 25th, 2014 in urban Shanghai, using a combination of one nano Condensation Nucleus Counter system (nCNC), one nano-Scanning Mobility Particle Sizer (SMPS), and one long-SMPS. Measurements of sulfur dioxide by an SO_2 analyzer with pulsed UV fluorescence technique allowed calculation of sulfuric acid proxy. In addition, concentrations of ammonia were recorded with a Differential Optical Absorption Spectroscopy (DOAS). During this 62-day campaign, 13 NPF events were identified with strong burst of sub-3 nm particles and subsequent fast growth of newly formed particles. The observed nucleation rate ($J_{1.34}$), formation rate of 3 nm particles (J_3), and condensation sink (CS) were 112.4-271.0 cm^{-3} s^{-1}, 2.3-19.2 cm^{-3} s^{-1}, and 0.030-0.10 s^{-1}, respectively. Subsequent cluster/nanoparticle growth showed a clear size dependence, with average values of $GR_{1.35\sim1.39}$, $GR_{1.39\sim1.46}$, $GR_{1.46\sim1.70}$, $GR_{1.70\sim2.39}$, $GR_{2.39\sim7}$, and $GR_{7\sim20}$ being 1.6±1.0, 1.4±2.2, 7.2±7.1, 9.0±11.4, 10.9±9.8, and 11.4±9.7 nm h^{-1}, respectively. Correlation between nucleation rate ($J_{1.34}$) and sulfuric acid proxy indicates that nucleation rate $J_{1.34}$ was proportional to a 0.65±0.28 power of sulfuric acid proxy, indicating that the nucleation of particles can be explained by the activation theory. Correlation between nucleation rate ($J_{1.34}$)

and gas-phase ammonia suggests that ammonia was associated with NPF events. The calculated sulfuric acid proxy was sufficient to explain the subsequent growth of 1.34-3 nm particles, but its contribution became smaller when the particle size grew. Qualitatively, NPF events in urban Shanghai likely occur on days with low levels of aerosol surface area, meaning the sulfuric acid proxy is only a valid predictor when aerosol surface area is low.

1 Introduction

Aerosol particles can influence climate directly and indirectly (Andreae and Crutzen, 1997; Haywood and Boucher, 2000; IPCC, 2013), and have adverse impact on human health (Dockery et al., 1993; Laden et al., 2006; Pope and Dockery, 2006). Atmospheric nucleation of gas-phase precursors to clusters, and then further to nanoparticles is the largest source of atmospheric aerosol particles (Kulmala et al., 2004; Zhang et al., 2012). This phenomenon has been observed in numerous locations around the world, including areas with a pristine atmosphere, e.g., coastal areas (O'Dowd et al., 2002), Antarctic/Arctic (Park et al., 2004), remote forest (Dal Maso et al., 2005), semi-rural locations with very low pollution levels such as Kent, OH (Kanawade et al., 2012), and heavily polluted cities, such as Mexico City (Dunn et al., 2004).

The exact mechanism for atmospheric nucleation is still under active investigation. Field measurements and laboratory studies have shown that sulfuric acid is a key precursor species for atmospheric nucleation (Weber et al., 1996; Sipila et al., 2010), and that atmospheric nucleation rate can be significantly promoted in presence of other precursors including ammonia (Ball et al., 1999; Benson et al., 2009), amines (Berndt et al., 2010; Zhao et al., 2011), and organic acids (Zhang et al., 2004; Zhang et al., 2009). At certain locations, ion-induced nucleation (Yu and Turco, 2001; Lee et al., 2003) or iodine species (O'Dowd et al., 2002) may also help to explain the observed new particle formation. Very recently progress has been made by the use of Particle Size Magnifier (PSM) and Chemical Ionization Atmospheric Pressure

interface Time-of-Flight (CI-APi-ToF) mass spectrometer, by combining the Cloud (Cosmics Leaving OUtdoor Droplets) chamber experiments and ambient observations including those at Hyytiälä, Finland, showing that oxidation products of biogenic emissions, together with sulfuric acid, contribute to new particle formation in the atmosphere (Schobesberger et al., 2013; Riccobono et al., 2014).

China suffers severe air pollution, especially high atmospheric particle loadings in recent years (Chan and Yao, 2008). Among many potential sources of atmospheric particles, atmospheric nucleation has been suggested to be a significant source of particles (Matsui et al., 2011; Yue et al., 2011). Correspondingly, a number of extensive campaign or long-term observational studies have been carried out in the Beijing area (e.g., Wu et al., 2007; Yue et al., 2009; Zhang et al., 2011; Gao et al., 2012) and Pearl River Delta, including Hong Kong (e.g., Guo et al., 2012; Yue et al., 2013). As one of the most industrialized area of China, one of the most populated region in the world, and one of the hotspots for particle pollution, Yangtze River Delta (YRD) has only seen a few research activities on atmospheric nucleation (Du et al., 2012; Herrmann et al., 2014). Among the few studies, measurements at the station for Observing Regional Processes of the Earth System, Nanjing University (SORPES-NJU) offered a first insight for new particle formation in the western part of YRD (Herrmann et al., 2014). On the other hand, atmospheric nucleation research in China is still in its infant stage and the latest experimental techniques are yet to be applied in China. For example, data on freshly nucleated particles are really sparse, except for those from an air ion spectrometer employed at SORPES-NJU (Herrmann et al., 2014). To the best of our knowledge, the use of a Particle Size Magnifier (PSM), which is able to study atmospheric nucleation at the size (mobility diameter) down to 1.5 ± 0.4 nm (Kulmala et al., 2012), has not been reported in a Chinese location in literature. The lack of key information greatly hinders a better understanding of nucleation mechanisms in China, where concentrations of sulfuric acid and basic gases including ammonia and amines are high (Zheng et al., 2011; Zheng et al., 2015) but concentrations of extremely low volatility organic compounds formed from

biogenic emissions are yet to be determined.

Direct measurements of atmospheric nucleation rates down to 1.5 ± 0.4 nm provide a better and more accurate characterization of atmospheric nucleation, since the indirect calculation of atmospheric nucleation rates from the formation rates of 3 nm particles leads to substantial uncertainty due to our incomplete understanding of condensational growth and coagulation scavenging of particles in the 1.5 to 3 nm range (Anttila et al., 2010; Korhonen et al., 2011). With the growing number of reports of real nucleation rates in clean atmosphere (e.g., Kulmala et al., 2012; Yu et al., 2014), it is ideal to measure nucleation rates in a polluted urban atmosphere to find out how atmospheric nucleation rates vary under different atmospheric conditions. In addition, the nucleation mechanism in a polluted urban atmosphere that is vital to understand atmospheric nucleation at a global scale and for atmospheric model development can be preliminarily investigated by examining the relationship between the measured atmospheric nucleation rates and the well-accepted precursor gases that exist in high concentrations.

In this study, we measured atmospheric nucleation from Nov. 25th, 2013 to Jan. 25th, 2014 in urban Shanghai with nCNC and two sets of SMPS. Nucleation frequency, nucleation rate ($J_{1.34}$), condensation sink (CS), and growth rates (GR) are reported and compared with previous studies with similar or dissimilar atmospheric environments. In addition, the potential nucleation mechanism was explored by correlating sulfuric acid proxy calculated from sulfur dioxide precursor and gas-phase ammonia to nucleation rate ($J_{1.34}$).

2 Experimental

2.1 Nucleation Measurements

Nucleation measurements were carried out on the rooftop of a teaching building (31°18’N, 121°30’E) that is about 20 m above ground on the campus of Fudan

University between Nov. 25th, 2013 and Jan. 25th, 2014. This monitoring site is mostly surrounded by commercial properties and residential dwellings. The Middle Ring Road, one of main overhead highways in Shanghai, lies about 100 m to the south of the site. Hence, the Fudan site can be treated as a representative urban site influenced by a wide mixture of emission sources (Wang et al., 2013; Ma et al., 2014).

Ambient particle size distributions in the range of 1.34-615 nm were measured using a combination of one nano Condensation Nucleus Counter system (model A11, Airmodus, Finland), one nano-SMPS (consisting of one DMA3085 and one CPC3776, TSI, USA), and one long-SMPS (consisting of one DMA3081 and one CPC3775, TSI, USA). The instruments were continuously running except for maintenance and minor instrument breakdown during the campaign.

Ambient air was drawn into a stainless steel manifold of 5.0 m length and 4 inch inner diameter at a flow rate of 153 CFM using a blower (Model DJT10U- 25M, NUSSUN, China). From this main manifold, 1.75 lpm ambient air was drawn through a 1/4 inch inner diameter stainless tube of 18 cm length, and diluted with a zero air flow generated by a zero air generator (Model 111, Thermo, USA) at a ratio of 1:1 to reduce the overall relative humidity (RH) and the number of particles entering PSM, since high RH and particle loading had an impact on the saturation of diethylene glycol in PSM and hence data quality. Subsequently 2.5 lpm diluted air was sampled into nCNC. In addition, 30 lpm split flow was drawn from the main manifold through a 1/4 inch inner diameter conductive silicon tubing of 50 cm length, and then 0.3 lpm and 1.5 lpm ambient air from the split flow, respectively, were drawn into nano-SMPS and long-SMPS. The calculated diffusion loss is up to 29% for 1.35 nm particles with the above setup, and has been taken into account in the entire size range during the data processing.

The nCNC system consists of one PSM (model A10, Airmodus, Finland) and one butanol Condensation Particle Counter (bCPC, model A20, Airmodus, Finland), and

was used to measure size distributions of 1.34-3 nm clusters/particles. Briefly, PSM activates the smallest particles using diethylene glycol as a working fluid and condensationally grows nanoparticles up to larger than 90 nm in mobility equivalent diameter, after which an external CPC is used for further growing the particles to optical sizes and counting the grown particles (Vanhanen et al., 2011). In this study, PSM was used in the scanning mode in which the saturator flow rate is changed continuously, giving an activation spectrum of the measured particles to obtain size distribution of sub-3 nm clusters/particles. A scanning cycle of 100 steps between saturator flow rates 0.1-1 lpm and a time resolution of 220 sec were chosen. Sub-3 nm clusters/particles were classified into 5 bins, i.e., 1.34-1.37, 1.37-1.41, 1.41-1.52, 1.52-1.89, 1.89-3.0 nm, respectively. Geometric mean values of upper and lower limits of the five bins, i.e., 1.35, 1.39, 1.46, 1.70, and 2.39 nm, respectively, were used to refer to the five bins in the growth rate calculation.

The nano-SMPS measured particles in the size range from 3 to 64 nm and the long-SMPS recorded particles from 14 to 615 nm. For both SMPSs, 64 size bins and 5-min time resolution were chosen. The sample flow to sheath flow ratios for both SMPSs were set at 1:10. A comparison analysis on the total particle concentrations between 14 and 64 nm measured by both nano-SMPS and long-SMPS showed less than 10% difference in the size range of 55-64 nm between two SMPSs. Hence, number concentrations of particles in the size range of 3-615 nm, $N_{3\sim615}$, were calculated from the sum of $N_{3\sim55}$ obtained from nano-SMPS, $N_{55\sim64}$ from the arithmetic average of nano-SPMS and long-SMPS, and $N_{64\sim615}$ from long-SMPS.

At the same site, sulfur dioxide (SO_2) was measured by an SO_2 analyzer with pulsed UV fluorescence technique (Model 43i, Thermo, USA) with a time resolution of 5 min and calibration of this SO_2 analyzer was performed every month. A DOAS system was used to measure the integrated concentration of NH_3 along the optical path between a transmitter telescope using a 35W Deuterium lamp as the light source and a receiver telescope (53 m), and then to yield the average concentration of NH_3

through dividing the integrated concentration by the absorption length (Platt and Stutz, 2008). In this study, the concentration of NH_3 was determined by fitting the reference spectra to the atmospheric spectra in a given window (205-220 nm) using a nonlinear least-squares method, similarly to a previous measurement of HONO and NO_2 (Wang et al., 2013). Detection limit of NH_3 was about 1 ppb with a 3 min integration time.

Solar radiation intensity measured by a Pyranometer (Kipp & Zonen CMP6, Netherland) was obtained from Shanghai Pudong Environmental Monitoring Centre (31°14'N, 121°32'E, about 8.78 km from the Fudan site).

2.2 Data Processing

2.2.1 Nucleation rate ($J_{1.34}$), formation rate of 3 nm particles (J_3), growth rate (GR), and condensation sink (CS)

In this study, PSM allowed measurements of clusters/particles down to 1.34 nm. Hence, atmospheric nucleation rate, $J_{1.34}$, defined as the flux of particles growing over 1.34 nm, can be calculated by taking into account the coagulation losses and condensational growth out of the considered size range (Kulmala et al., 2012),

$$J_{1.34} = \frac{dN_{1.34\sim3}}{dt} + CoagS_{d_p=2nm} \cdot N_{1.34\sim3} + \frac{1}{1.66nm} GR_{1.34\sim3} \cdot N_{1.34\sim3} \quad (1)$$

where $CoagS_{d_p=2nm}$ represents coagulation sink of 2 nm particles, an approximation for that in the size interval of 1.34-3 nm; and $GR_{1.34\sim3}$ represents the apparent clusters/particle growth rate between 1.34 and 3 nm.

Formation rate of 3nm particles was calculated in a similar way (Sihto et al., 2006; Kulmala et al., 2012), providing a comparison with previous studies,

$$J_3 = \frac{dN_{3\sim6}}{dt} + CoagS_{d_p=4nm} \cdot N_{3\sim6} + \frac{1}{3nm} GR_{3\sim6} \cdot N_{3\sim6} \quad (2)$$

where $CoagS_{d_p=4nm}$ represents coagulation sink of 4 nm particles, an approximation for that in the size interval of 3-6 nm.

Growth rate (GR) is defined as the rate of change in the diameter of a growing

particle population, using the maximum-concentration method (Kulmala et al., 2012),

$$GR = \frac{dd_p}{dt} = \frac{\Delta d_p}{\Delta t} = \frac{d_{p_2} - d_{p_1}}{t_2 - t_1} \quad (3)$$

where d_{p_1} and d_{p_2} are the representative particle diameters at times t_1 and t_2, respectively.

Condensation sink (CS) describes the condensing vapor sink caused by the particle population (Kulmala et al., 2012),

$$CS = 4\pi D \int_0^{d_p \max} \beta_{m,d_p} d_p N_{d_p} dd_p = 4\pi D \sum_{d_p} \beta_{m,d_p} d_p N_{d_p} \quad (4)$$

where D is the diffusion coefficient of the condensing vapor, usually assumed to be sulfuric acid (0.104 $cm^2\ s^{-1}$ used in this study); and β_{m,d_p} is the transitional regime correction factor.

2.2.2 Sulfuric acid

Sulfuric acid has been accepted as a key gas-phase precursor for atmospheric nucleation and contributes to the subsequent growth of newly-formed particles (Weber et al., 1996; Sipila et al., 2010). The accurate measurement of gas-phase sulfuric acid requires application of chemical ionization mass spectrometry using nitrates as reagent ions (Eisele and Tanner, 1993), which is not possessed by this research group during this study. Instead, the sulfuric acid proxy $[H_2SO_4]$ was estimated based on local solar radiation level *Radiation* , SO_2 concentration $[SO_2]$, condensation sink CS, and relatively humidity (Mikkonen et al., 2011),

$$[H_2SO_4] = 8.21 \times 10^{-3} \cdot k \cdot Radiation \cdot [SO_2]^{0.62} \cdot (CS \cdot RH)^{-0.13} \quad (5)$$

where k is the temperature dependent reaction rate constant. The relative error between calculated sulfuric acid proxy and measured sulfuric acid concentration is estimated to be 42% (Mikkonen et al., 2011). The time resolution of calculated sulfuric acid proxy was 1 hour since those of temperature and relative humidity was 1 hour.

Condensation of sulfuric acid contributes to the growth of newly-formed particles. The growth of clusters/particles due to condensation of sulfuric acid, $GR_{H_2SO_4}$, can be estimated by the following equations (Nieminen et al., 2010),

$$GR_{H_2SO_4} = \frac{\gamma}{2\rho_v}\left(1+\frac{d_v}{d_p}\right)^2\left(\frac{8kT}{\pi}\right)^{1/2}\left(\frac{1}{m_p}+\frac{1}{m_v}\right)^{1/2} m_v[H_2SO_4] \quad (6)$$

and $$\gamma = \frac{4}{3}\cdot Kn\cdot \beta_{m,d_p} \quad (7)$$

where ρ_v and d_v are the condensed phase density and molecule diameter of H_2SO_4, respectively; m_p and m_v are particle and H_2SO_4 vapor molecule masses, respectively; γ is a correction factor; Kn is the Knudsen number (Lehtinen and Kulmala, 2003). For this calculation, particle density ρ_p = 1.83 g cm^{-3} was used.

The particle growth due to the hydration of H_2SO_4 is taken into account by assuming that sulfuric acid is instantaneously equilibrated with gas-phase water. During our campaign, daily average RH varied between 28.7%~60.0%. Hence, using the H_2SO_4-hydrate distribution data given by Kurtén et al. (2007), the density and mass of the average hydrated H_2SO_4 molecule at 50% relative humidity is calculated and further used in equation (6).

3 Results and Discussion

3.1 Classification of new particle formation (NPF) events

Figure 1 presents a contour plot for particle size distributions of 3-615 nm and a number concentration plot of sub-3 nm clusters/particles $N_{1.34\sim3}$ during Nov. 25th, 2013 - Jan. 25th, 2014. Data were occasionally missing because of maintenance and minor breakdown of instruments. From the figure, frequent bursts of sub-3 nm particles were evident, with concentrations up to 8.0 × 10^4 cm^{-3} around noon time. However, similarly to previous studies (Kulmala et al., 2007; Kulmala et al., 2013; Yu et al., 2014), not all sub-3 nm particles eventually underwent a continuous growth to

larger sizes. In this study, we define an observation day with appearances of sub-3 nm clusters/particles over a time span of hours and subsequent growth to larger sizes for a few hours as a NPF event day. In this case, a NPF day will present a banana-shaped contour plot of particle size distributions obtained from SMPS (Dal Maso et al., 2005). We focus on characteristics and potential mechanisms of these events.

According to the classification, there were 13 event days during the 62-day campaign, as illustrated by the shadow in Figure 1. Although nCNC data were partially unavailable on Dec. 26th, 2013 and completely unavailable on Jan. 24th, 2014, these two days are still defined as NPF days since a distinctive banana-shaped contour plot for particle distributions between 3-615 nm existed. Dec. 18th, 2013 was not regarded as a NPF day since $N_{1.34\sim3}$ was not recorded and the growth of 3~20 nm particles was relatively short-lived.

Among these NPF events, 5 NPF events occurred in November, 3 in December, and 5 in January. The averaged frequency for NPF events was 21.0% during the 62-day campaign. Our NPF frequency at Shanghai is larger than the average value in winter 1996-2003, SMEAR II station, Hyytiälä, Finland (Dal Maso et al., 2005), likely because nucleation events at Hyytiälä have recently been related to oxidation products of biogenic emissions (Kulmala et al., 1998; Schobesberger et al., 2013; Riccobono et al., 2014) and photochemistry of volatile organic compounds is less intensive in winter months. This frequency is also higher than that in winter, semi-rural Kent, OH, during which transport of sulfur dioxide from the east-southeast power plant to Kent is not favored (Kanawade et al., 2012). NPF events occurred at a frequency of around 40% during Nov.-Dec. 2004 in Beijing (Wu et al., 2007), much more often than in Shanghai. On the other hand, NPF frequency in Shanghai is remarkably close to that measured in winter 2012, Nanjing, which is also located in Yangtze River delta (Herrmann et al., 2014).

Number concentrations of particles in different size ranges, i.e., $N_{1.34\sim3}$, $N_{3\sim7}$, and $N_{7\sim30}$, respectively, on a NPF day (Dec. 11th, 2013) and an obvious non-NPF day (Jan. 7th, 2014) are further examined to illustrate features of a NPF event, as shown in Figure 2. On the NPF day, 1.34-3 nm particles appeared as early as 7 am in the morning that was right after sunrise (6:42 am on Dec. 11th, 2013), reached its maximum just before noontime, and spanned for almost the whole daytime (sunset at 4:52 pm, Dec. 11th, 2013), suggesting that photochemistry products likely contribute to formation of smallest particles. This size distribution of atmospheric neutral and charged clusters/particles by a scanning PSM is identical to that measured at Hyytiälä, Finland (Kulmala et al., 2013). On the same NPF day, 3-7 nm and 7-30 nm particles appeared much later, resembling previous findings only with SMPS measurements (e.g., Yue et al., 2010). The lag in peaking times of $N_{1.34\sim3}$, $N_{3\sim7}$, and $N_{7\sim30}$ on the NPF day clearly indicated the continuous growth of clusters/particles, the reduction of particles due to coagulation during the growth, and the diverse sources of particles in the size range of 7-30 nm. In contrast, $N_{1.34\sim3}$ and $N_{3\sim7}$ showed a flat profile on the non-NPF day. The minor enhancement in $N_{7\sim30}$ between 10 am and 5 pm on the non-NPF day was not due to growth of newly formed particles. Instead, direct emission of 7-30 nm particles from transportation activity likely explained their appearance.

3.2 General characteristics of NPF events

Table 1 summaries characteristics of each NPF event observed in this campaign, including $J_{1.34}$, J_3, $GR_{1.35\sim2.39}$ (from the bin of 1.34-1.37 nm to the bin of 1.89-3.0 nm), $GR_{2.39\sim7}$, $GR_{7\sim20}$, CS, $[H_2SO_4]$, $N_{1.34\sim3}$, and total number concentrations of particles $N_{1.34\sim615}$, and compares the mean values to those in selected other studies. Nucleation rate $J_{1.34}$ and formation rate of 3 nm particles J_3 were 112.4-271.0 and

2.3-19.2 cm^{-3} s^{-1}, respectively. Nucleation rate $J_{1.34}$ at Shanghai is obviously significantly larger than 1.4 cm^{-3} s^{-1} at Hyytiälä, Finland with a pristine atmosphere (Kulmala et al., 2012) and 1.3 cm^{-3} s^{-1} at Kent, OH with relatively lower levels of pollutants (Yu et al., 2014). Direct comparison of our nucleation rate with that in a Chinese location is not feasible because no previous reports are available. However, Herrmann et al. (2014) reported a J_2 of 33.2 cm^{-3} s^{-1} at the SORPES-NJU station, Nanjing China. Together with their results, we conclude that strong nucleation events occur geographically widely in the YRD region.

Formation rate of 3 nm particles J_3 has been more routinely reported. Similarly to $J_{1.34}$, J_3 at Shanghai is significantly larger than 0.61 cm^{-3} s^{-1} at Hyytiälä, Finland (Kulmala et al., 2012), and generally comparable to 3.3-81.4 and 1.1-22.4 cm^{-3} s^{-1} at Beijing (Wu et al., 2007; Yue et al., 2009), 3.6-6.9 cm^{-3} s^{-1} at Hong Kong (Guo et al., 2012), and 2.4-4.0 cm^{-3} s^{-1} in a back-garden rural site of Pearl River Delta (Yue et al., 2013). The fast reduction from $J_{1.34}$ to J_3 was likely due to the presence of a large background particle number as shown in Table 1.

The large background particle number concentrations corresponded to the high condensation sink (*CS* of 0.030-0.10 s^{-1}) observed during the campaign. As shown in Table 1, *CS* at Shanghai is much larger than $(0.05\text{-}0.35)\times10^{-2}$ s^{-1} at Hyytiälä, Finland (Kulmala et al., 2012) and 0.8×10^{-2} s^{-1} at Kent, OH (Yu et al., 2014), but comparable to $(0.58\text{-}8.4)\times10^{-2}$ s^{-1} at Beijing (Wu et al., 2007; Yue et al., 2009; Zhang et al., 2011; Gao et al., 2012), $(1.0\text{-}6.2)\times10^{-2}$ s^{-1} at Hong Kong (Guo et al., 2012), 2.4×10^{-2} s^{-1} at Nanjing (Herrmann et al., 2014) , and $(3.5\text{-}4.6)\times10^{-2}$ s^{-1} in an urban site of Pearl River Delta (Yue et al., 2013). High sulfuric acid proxy ($[H_2SO_4]$ of $(2.3\text{-}6.4)\times10^7$ molecules cm^{-3}) existed to promote the NPF events. Measurements of gas-phase sulfuric acid by a chemical ionization mass spectrometer during the CAREBeijing 2008 Campaign, a time period with strict air quality control regulations, reported peak

concentrations of sulfuric acid up to the order of 10^7 molecules cm^{-3} (Zheng et al., 2011), smaller than our sulfuric acid proxy. Uncertainty may well exist for our sulfuric acid proxy that was calculated from the concentrations of sulfur dioxide and radiation intensity. However, Judging from CS and $[H_2SO_4]$ together, it is clear that the condensable vapor at Shanghai is likely a main impetus for observed strong new particle formation events.

$GR_{1.35\sim2.39}$, $GR_{2.39\sim7}$, and $GR_{7\sim20}$ were in the range of 0.49-8.1, 3.1-35.7, 4.5-38.3 nm h^{-1}, respectively. The arithmetic average values of $GR_{1.35\sim2.39}$, $GR_{2.39\sim7}$, and $GR_{7\sim20}$ were 2.0 ± 2.7 (one standard deviation), 10.9 ± 9.8 and 11.4 ± 9.7 nm h^{-1}, respectively, which are comparable to 3-20 nm h^{-1} for nucleation mode particles in another sulfur-rich city, Atlanta, GA (Stolzenburg et al., 2005). In addition, $GR_{1.35\sim2.39}$ at Shanghai is smaller than the growth rates (5.5-7.6 nm h^{-1}) for particles in 1~3 nm geometric diameter range in Atlanta (Kuang et al., 2012). A closer examination of growth rates was performed by dividing $GR_{1.35\sim2.39}$ into growth of clusters/particles from one bin to another, i.e., $GR_{1.35\sim1.39}$ (1.6 ± 1.0 nm h^{-1} from the bin of 1.34-1.37 nm to the bin of 1.37-1.41 nm), $GR_{1.39\sim1.46}$ (1.4 ± 2.2 nm h^{-1} from 1.37-1.41 nm to 1.41-1.52 nm), $GR_{1.46\sim1.70}$ (7.2 ± 7.1 nm h^{-1} from 1.41-1.52 nm to 1.52-1.89 nm), and $GR_{1.70\sim2.39}$ (9.0 ± 11.4 nm h^{-1} from 1.52-1.89 nm to 1.89-3.0 nm). These growth rates show a clear size-dependent particle growth (Fig.3), owing to the nano-Köhler activation that suggests a faster growth for activated nanoparticles due to a decreasing Kelvin effect and, thus, an enhanced condensation flux (Kulmala et al., 2004), Kelvin effect, and surface or volume-controlled reaction corrected for the Kelvin effect on surface or volume concentrations (Kuang et al., 2012) . Similar observations have been reported in previous studies using nCNC (Kulmala et al., 2013) and DEG UCPC (Kuang et al., 2012), respectively. Our $GR_{2.39\sim7}$ is larger than 6.3 nm h^{-1} at Nanjing (Herrmann et al.,

2014), and our $GR_{7\sim20}$ is close to the upper bound of those at urban Beijing (Wu et al., 2007; Yue et al., 2009; Zhang et al., 2011; Gao et al., 2012), and generally larger than 1.5-8.4 nm h^{-1} in Hong Kong (Guo et al., 2012), indicating that high concentrations of condensable vapors existed. In addition, our growth rates suggest that the smallest clusters (the bin of 1.34-1.37 nm), if not scavenged by larger particles, would grow to 3 nm within ~12 min, and to 20 nm within ~2 hr.

3.3 Potential mechanisms for NPF events

As shown in Table 1, nucleation rate ($J_{1.34}$) in this study is typically larger than 100 cm^{-3} s^{-1}, suggesting that the ion-induced nucleation was not a main mechanism for observed fast nucleation (Hirsikko et al., 2011; Riccobono et al., 2014). The 2012 winter study at the SORPES-NJU station that is also located at YRD shows that the ratio of J_2 between ions and total particles (ions plus neutral particles) was 0.002, also indicating the minor role of ion-induced nucleation (Herrmann et al., 2014). Hence, it is likely that nucleation of neutral precursor molecules actually largely determined the observed NPF events.

Correlations between $\log J_{1.34}$ and $\log[H_2SO_4]$ (Figure 4) and between $\log J_{1.34}$ and $\log[NH_3]$ (Figure 5) were examined to elucidate potential mechanisms for our NPF events. Since $J_{1.34}$ could not be accurately determined on some of the NPF days, the number of data points in both figures was less than the actual number of NPF events that have been observed. Daily peak concentration of sulfuric acid proxy and daytime (6 am – 6 pm) averages of ammonia were used as approximations for their effective concentrations on a NPF day since there was no peak concentration for ammonia. The correlation (R^2=0.62) between $\log J_{1.34}$ and $\log[NH_3]$ is better than that (R^2=0.38) between $\log J_{1.34}$ and $\log[H_2SO_4]$, and slopes are 0.57 ± 0.17 and 0.65 ± 0.28, respectively.

Most ambient studies showed that nucleation rate J is proportional to the first or second power of the concentration of gas-phase sulfuric acid, i.e., $J = A \cdot [H_2SO_4]^p$, where P is equal to 1 or 2, conventionally interpreted as the number of sulfuric acid molecules in the critical nucleus, and A is a pre-exponential factor (McMurry et al., 2005; Sihto et al., 2006; Erupe et al., 2010). Our P of 0.65 ± 0.28 is of a significant uncertainty, which could come from the uncertainty during the calculation of sulfuric acid proxy $[H_2SO_4]$ and the scarcity of our data points. The upper limit of our P indicates that nucleation occurs after activation of clusters containing one molecule of sulfuric acid, with subsequent growth involving other species (Kulmala et al., 2006). The lower limit, on the other hand, would imply a less important role of sulfuric acid in the critical nucleus during our campaign, which is unlikely to be true according to numerous previous studies (Weber et al., 1996; Sipila et al., 2010; Yu and Hallar, 2014). Kupiainen-Määttä, et al. (2014) recently reported that the number of molecules in a critical cluster cannot be determined by a slope analysis in atmospherically relevant applications, underscoring the need to further explore the exact nucleation mechanism. Herrmann et al., (2014) also calculated the sulfuric acid proxy, related it to observed nucleation rates, and speculated that the sulfuric acid exponent might be well over 2, which underscores the reliability of calculation methods in a Chinese location. Hence, our preliminary result should be further tested with actual measurements of gas-phase sulfuric acid, but does indicate the key role of sulfuric acid in NPF events. On the other hand, linear correlation between $\log J$ and $\log[NH_3]$ was observed in a previous nucleation study in Atlanta, GA, with a slope of 1.17 (McMurry et al., 2005), but a clear relationship was not perceived at Kent, OH (Erupe et al., 2010). This discrepancy may come from the level of ammonia that has been predicted to have a saturation threshold (Napari et al., 2002) and/or the co-existing sulfuric acid concentration (Benson et al., 2009). Nevertheless, our correlation between $\log J$ and $\log[NH_3]$ suggests that ammonia also participated in

the nucleation. A recent CIMS study (Zheng et al., 2015) observed good correlations between NH_3 and amines at an urban site of Nanjing, China. Hence, it is plausible that amines may contribute to nucleation in our site at Shanghai, too.

The subsequent growth of newly formed particles can be partially attributed to condensation of sulfuric acid. The theoretical maximum growth rate of 1.34-3 nm clusters/particles due to condensation of hydrated sulfuric acid at 50% RH ($GR_{H_2SO_4(1.34\sim3)}$), calculated according to eq. 6 and 7, was 3.9 ± 1.3 nm h^{-1} on average. This rate is larger than the observed growth rates of clusters/particles from the bin of 1.34-1.37 nm to the bin of 1.89-3.0 nm ($GR_{1.35\sim2.39}$), being 2.0 ± 2.7 nm h^{-1}, indicating that sulfuric acid proxy was enough to explain the observed growth for particles under 3 nm. Similar calculation of $GR_{H_2SO_4(3\sim7)}$ and $GR_{H_2SO_4(7\sim20)}$ yielded 2.8 ±0.94 and 2.2 ± 0.74 nm h^{-1}, respectively. In figure 6, relative contributions of sulfuric acid to growth of particles in the range of 3-7 and 7-20 nm, respectively, on each NPF day is presented. Since 7 nm particles reached their maximum earlier than 3 nm particles on Jan. 9th and Jan. 15th, 2014, there was no calculated $GR_{3\sim7}$ and hence no ratios available on these two days. In addition, condensation of hydrated sulfuric acid was more prominent for 3-7 nm particles on 6 NPF days (Nov. 25th, Nov. 26th, Nov. 30th, Dec. 10th, Dec. 11th, and Dec. 12th 2013), whereas it was more significant for 7-20 nm particles on the other 5 NPF days (Nov. 28th 2013, Nov. 29th 2013, Jan. 13th 2014, Jan. 21st 2014, and Jan. 24th 2014). On average, condensation of gas-phase hydrated sulfuric acid explained 39.1% of $GR_{2.39\sim7}$, and 29.0% of $GR_{7\sim20}$, respectively. The rest of growth might be largely attributed to condensation of extremely low volatility organic compounds (Ehn et al., 2014), and potentially heterogeneous reactions of organics on nanoparticle surface (Wang et al., 2010; Wang et al., 2011).

3.4 NPF and Aerosol Surface Area

NPF events in urban environment are of special interests since the pre-existing

particle surface may significantly scavenge the newly formed particles and change the probability of NPF. We plot number concentrations of 1.34-10 nm particles ($N_{1.34\sim10}$), sulfuric acid proxy ($[H_2SO_4]$), ammonia ($[NH_3]$), and aerosol surface area with shadowed blocks representing NPF events in Figure 7. Note that $N_{1.34\sim10}$ was used as an approximation for nucleation and subsequent growth while excluding particles from direct emission. The average daytime (6 am-6 pm) $N_{1.34\sim10}$ on NPF days was $(2.7\pm2.1)\times10^4$ cm^{-3}, much larger than $(1.5\pm1.0)\times10^4$ cm^{-3} on the rest days of the campaign, indicating that a stronger input of particles from nucleation processes on NPF days. However, daytime $[H_2SO_4]$ did not show an apparent difference between on NPF days ($(3.7\pm1.2)\times10^7$ molecules cm^{-3}) and on the rest days ($(3.9\pm2.5)\times10^7$ molecules cm^{-3}). For example, an episode with high daily sulfuric acid proxy during Dec. 19th, 2013 and Jan. 16th, 2014 did not lead to any NPF events. Instead, observed NPF events occurred on days with low aerosol surface area levels and moderate $[H_2SO_4]$. During our campaign, NPF days were characterized with low aerosol surface area ($(7.8\pm3.8)\times10^8$ nm^2 cm^{-3}), whereas the average was $(10.4\pm4.7)\times10^8$ nm^2 cm^{-3} on the rest days of the campaign. Ammonia varied dramatically, even within a single day. NPF events occurred on days with around 10-fold difference in ammonia concentrations. According to ammonia's profile and its positive correlation with $J_{1.34}$, we speculate that ammonia was involved in nucleation but it is not the driving force.

Examination of these parameters from Jan. 12th to Jan. 14th, 2014 was performed since the three days were characterized with similar meteorological conditions. The average daytime concentration of sulfuric acid proxy was 2.8, 2.3, and 1.0 $\times10^7$ molecules cm^{-3} on Jan. 12th, 13th and 14th, 2014, respectively. No NPF event was observed on Jan. 14th at least partially because of the low sulfuric acid proxy. Appearance of a NPF event on Jan. 13th and non-appearance on Jan, 12th could be explained by the high aerosol surface area on Jan. 12th, with maximum aerosol surface area up to 1.8×10^9

483 nm^2 cm^{-3}, although similar sulfuric acid proxies existed between the two days. Hence,
484 we conclude that, qualitatively, NPF processes in urban Shanghai occurred with low
485 levels of aerosol surface and that high sulfuric acid favored NPF events when aerosol
486 surface area was low. This conclusion is identical to that drawn from a Mexico City
487 study where NPF events observed in the city correlated with elevated concentrations
488 of sulfur dioxide and low particulate matter mass concentrations in the afternoon
489 hours (Dunn et al., 2004).
490
491 **4 Summary and Conclusions**
492 Atmospheric new particle formation is a significant source of atmospheric aerosol
493 particles. Understanding NPF under the current levels of air pollution in China is of
494 special scientific interests because the exact nucleation mechanism under urban
495 environment remains elusive. From Nov. 25th, 2013 to Jan. 25th, 2014, a combination
496 of one nano-CNC, one nano-SPMS, and one long-SPMS has been utilized to
497 investigate atmospheric nucleation by measuring particle size distributions in the
498 range of 1.34-615 nm at urban Shanghai, located in the east Yangtze River Delta.
499 During this 62-day campaign, 13 NPF events were identified with strong burst of sub-
500 3 nm particles and subsequent fast growth of newly formed particles. Together with
501 nucleation frequency (21%), the obtained nucleation rate $J_{1.34}$ (112.4-271.0 cm^{-3} s^{-1}),
502 condensation sink *CS* (0.030-0.10 s^{-1}), and aerosol surface area ((7.8±3.8) $\times 10^8$ nm^2
503 cm^{-3}) on NPF event days clearly indicate that strong atmospheric new particle
504 formation occurred in winter, urban Shanghai with competition between promotion
505 from condensable vapors and scavenging by preexisting particles. The absolute values
506 of $J_{1.34}$ and *CS* are one to two orders of magnitude lager than those at locations with a
507 pristine atmosphere (e.g., Kulmala et al., 2012) and semi-rural locations with very low
508 pollution levels such as Kent, OH (Yu et al., 2014), as a reflection from the
509 significantly-altered atmospheric background.
510
511 Our preliminary exploration on nucleation mechanism indicates that nucleation rate

$J_{1.34}$ was proportional to a 0.65 ± 0.28 power of sulfuric acid proxy. It is hence likely that observed NPF events could be explained by the activation theory. As Herrmann et al., (2014) doubted reliability of sulfuric acid proxy, accurate measurements of gas-phase sulfuric acid instead of calculation of a proxy is necessary to achieve an unambiguous conclusion. The positive correlation between $J_{1.34}$ and gas-phase ammonia hints the involvement of ammonia in new particle formation, but its exact role cannot be determined without measurements of nucleating clusters, either.

A size-depend particle growth in the range of 1.34-20 nm has been observed in this study, consistent with predictions from nano-Köhler theory (Kulmala et al., 2004), and Kelvin-limited diffusion, surface, and volume growth laws (Kuang et al., 2012). Sulfuric acid proxy was enough to explain the observed growth for particles under 3 nm, and contributed to 39.1% of $GR_{2.39\sim7}$, and 29.0% of $GR_{7\sim20}$, respectively. The rest of growth could be largely attributed to condensation of extremely low volatility organic compounds (Ehn et al., 2014), and potentially heterogeneous reactions of organics on nanoparticle surface (Wang et al., 2010; Wang et al., 2011).

Clearly, further long term measurements with integrated state-of-the-art measurement techniques are necessary to draw a comprehensive picture of atmospheric nucleation events in China. Currently, atmospheric sub-3 nm particle measurements are still scarce in China, not mentioning measurements of gas-phase sulfuric acid, nucleating clusters, and other potential precursors. Nevertheless, our study offers a very first measurement of sub-3 nm particles in urban Shanghai, and provides some of the preliminary mechanisms for NPF events in China.

Acknowledgments

This study was financially supported by National Natural Science Foundation of China (No. 21107015, 21190053, 21277029 & 21222703), Ministry of Science & Technology of China (2012YQ220113-4), Science & Technology Commission of

Shanghai Municipality (12DJ1400100), and Cyrus Tang Foundation. LW thanks the Jiangsu Provincial 2011 Program (Collaborative Innovation Centre of Climate Change).

References:

Andreae, M. O., and Crutzen, P. J.: Atmospheric aerosols: Biogeochemical sources and role in atmospheric chemistry, Science, 276, 1052-1058, 1997.

Anttila, T., Kerminen, V.-M., and Lehtinen, K. E. J.: Parameterizing the formation rate of new particles: The effect of nuclei self-coagulation, Journal of Aerosol Science, 41, 621-636, 10.1016/j.jaerosci.2010.04.008, 2010.

Ball, S., Hanson, D., Eisele, F., and McMurry, P.: Laboratory studies of particle nucleation: Initial results for H_2SO_4, H_2O, and NH_3 vapors, Journal of Geophysical Research: Atmospheres (1984–2012), 104, 23709-23718, 1999.

Benson, D. R., Erupe, M. E., and Lee, S. H.: Laboratory-measured H_2SO_4-H_2O-NH_3 ternary homogeneous nucleation rates: Initial observations, Geophysical Research Letters, 36, L15818, doi: 10.1029/2009GL038728, 2009.

Berndt, T., Stratmann, F., Sipilä, M., Vanhanen, J., Petäjä, T., Mikkilä, J., Grüner, A., Spindler, G., Mauldin III, L., and Curtius, J.: Laboratory study on new particle formation from the reaction OH+ SO_2: influence of experimental conditions, H_2O vapour, NH_3 and the amine tert-butylamine on the overall process, Atmospheric Chemistry and Physics, 10, 7101-7116, 2010.

Chan, C. K., and Yao, X.: Air pollution in mega cities in China, Atmospheric Environment, 42, 1-42, 2008.

Dal Maso, M. D., Kulmala, M., Riipinen, I., Wagner, R., Hussein, T., Aalto, P. P., and Lehtinen, K. E.: Formation and growth of fresh atmospheric aerosols: eight years of aerosol size distribution data from SMEAR II, Hyytiälä, Finland, Boreal Environment Research, 10, 323-336, 2005.

Dockery, D. W., Pope, C. A., Xu, X., Spengler, J. D., Ware, J. H., Fay, M. E., Ferris Jr, B. G., and Speizer, F. E.: An association between air pollution and mortality in six US cities, New England journal of medicine, 329, 1753-1759, 1993.

Du, J., Cheng, T., Zhang, M., Chen, J., He, Q., Wang, X., Zhang, R., Tao, J., Huang, G., and Li, X.: Aerosol Size Spectra and Particle Formation Events at Urban Shanghai in Eastern China, Aerosol Air Qual. Res, 12, 1362-1372, 2012.

Dunn, M. J., Jiménez, J. L., Baumgardner, D., Castro, T., McMurry, P. H., and Smith, J. N.: Measurements of Mexico City nanoparticle size distributions: Observations of new particle formation and growth, Geophysical Research Letters, 31, L10102, doi:10.1029/2004GL019483, 2004.

Ehn, M., Thornton, J. A., Kleist, E., Sipilä, M., Junninen, H., Pullinen, I., Springer, M., Rubach, F., Tillmann, R., and Lee, B.: A large source of low-volatility secondary organic aerosol, Nature, 506, 476-479, 2014.

Eisele, F., and Tanner, D.: Measurement of the gas phase concentration of H_2SO_4 and methane sulfonic acid and estimates of H_2SO_4 production and loss in the atmosphere, Journal of Geophysical Research: Atmospheres (1984–2012), 98, 9001-9010, 1993.

Erupe, M. E., Benson, D. R., Li, J., Young, L.-H., Verheggen, B., Al-Refai, M., Tahboub, O., Cunningham, V., Frimpong, F., Viggiano, A. A., and Lee, S.-H.: Correlation of aerosol nucleation rate with sulfuric

583 acid and ammonia in Kent, Ohio: An atmospheric observation, Journal of Geophysical Research,
584 115, D23216, doi:10.1029/2010jd013942, 2010.
585 Gao, J., Chai, F., Wang, T., Wang, S., and Wang, W.: Particle number size distribution and new particle
586 formation: New characteristics during the special pollution control period in Beijing, Journal of
587 Environmental Sciences, 24, 14-21, 10.1016/s1001-0742(11)60725-0, 2012.
588 Guo, H., Wang, D. W., Cheung, K., Ling, Z. H., Chan, C. K., and Yao, X. H.: Observation of aerosol size
589 distribution and new particle formation at a mountain site in subtropical Hong Kong, Atmospheric
590 Chemistry and Physics, 12, 9923-9939, 10.5194/acp-12-9923-2012, 2012.
591 Haywood, J., and Boucher, O.: Estimates of the direct and indirect radiative forcing due to tropospheric
592 aerosols: A review, Reviews of Geophysics, 38, 513, 10.1029/1999rg000078, 2000.
593 Herrmann, E., Ding, A., Kerminen, V.-M., Petäjä, T., Yang, X., Sun, J., Qi, X., Manninen, H., Hakala, J.,
594 and Nieminen, T.: Aerosols and nucleation in eastern China: first insights from the new SORPES-
595 NJU station, Atmospheric Chemistry and Physics, 14, 2169-2183, 2014.
596 Hirsikko, A., Nieminen, T., Gagné, S., Lehtipalo, K., Manninen, H., Ehn, M., Horrak, U., Kerminen, V.-M.,
597 Laakso, L., and McMurry, P.: Atmospheric ions and nucleation: a review of observations,
598 Atmospheric Chemistry and Physics, 11, 767-798, 2011.
599 IPCC: IPCC, 2013: Climate change 2013: The physical science basis, Contribution of working group I to
600 the fourth assessment report of the intergovernmental panel on climate change Cambridge
601 University Press, Cambridge, United Kingdom and New York, NY, USA, 2013.
602 Kanawade, V. P., Benson, D. R., and Lee, S.-H.: Statistical analysis of 4-year observations of aerosol sizes
603 in a semi-rural continental environment, Atmospheric Environment, 59, 30-38,
604 10.1016/j.atmosenv.2012.05.047, 2012.
605 Korhonen, H., Sihto, S. L., Kerminen, V. M., and Lehtinen, K. E. J.: Evaluation of the accuracy of analysis
606 tools for atmospheric new particle formation, Atmospheric Chemistry and Physics, 11, 3051-3066,
607 10.5194/acp-11-3051-2011, 2011.
608 Kuang, C., Chen, M., Zhao, J., Smith, J., McMurry, P. H., and Wang, J.: Size and time-resolved growth
609 rate measurements of 1 to 5 nm freshly formed atmospheric nuclei, Atmospheric Chemistry and
610 Physics, 12, 3573-3589, 10.5194/acp-12-3573-2012, 2012.
611 Kulmala, M., Toivonen, A., Mäkelä, J. M., and Laaksonen, A.: Analysis of the growth of nucleation
612 mode particles observed in Boreal forest, Tellus B, 50, 449-462, 1998.
613 Kulmala, M., Kerminen, V. M., Anttila, T., Laaksonen, A., and O'Dowd, C. D.: Organic aerosol formation
614 via sulphate cluster activation, Journal of Geophysical Research: Atmospheres (1984–2012), 109,
615 D04205, doi: 10.1029/2003JD003961, 2004.
616 Kulmala, M., Vehkamäki, H., Petäjä, T., Dal Maso, M., Lauri, A., Kerminen, V. M., Birmili, W., and
617 McMurry, P. H.: Formation and growth rates of ultrafine atmospheric particles: a review of
618 observations, Journal of Aerosol Science, 35, 143-176, 10.1016/j.jaerosci.2003.10.003, 2004.
619 Kulmala, M., Lehtinen, K., and Laaksonen, A.: Cluster activation theory as an explanation of the linear
620 dependence between formation rate of 3nm particles and sulphuric acid concentration,
621 Atmospheric Chemistry and Physics, 6, 787-793, 2006.
622 Kulmala, M., Riipinen, I., Sipilä, M., Manninen, H. E., Petäjä, T., Junninen, H., Dal Maso, M., Mordas, G.,
623 Mirme, A., and Vana, M.: Toward direct measurement of atmospheric nucleation, Science, 318, 89-
624 92, 2007.
625 Kulmala, M., Petäjä, T., Nieminen, T., Sipilä, M., Manninen, H. E., Lehtipalo, K., Dal Maso, M., Aalto, P.
626 P., Junninen, H., Paasonen, P., Riipinen, I., Lehtinen, K. E. J., Laaksonen, A., and Kerminen, V.-M.:

627 Measurement of the nucleation of atmospheric aerosol particles, Nature Protocols, 7, 1651-1667,
628 10.1038/nprot.2012.091, 2012.
629 Kulmala, M., Kontkanen, J., Junninen, H., Lehtipalo, K., Manninen, H. E., Nieminen, T., Petaja, T., Sipila,
630 M., Schobesberger, S., Rantala, P., Franchin, A., Jokinen, T., Jarvinen, E., Aijala, M., Kangasluoma, J.,
631 Hakala, J., Aalto, P. P., Paasonen, P., Mikkila, J., Vanhanen, J., Aalto, J., Hakola, H., Makkonen, U.,
632 Ruuskanen, T., Mauldin, R. L., Duplissy, J., Vehkamaki, H., Back, J., Kortelainen, A., Riipinen, I.,
633 Kurten, T., Johnston, M. V., Smith, J. N., Ehn, M., Mentel, T. F., Lehtinen, K. E. J., Laaksonen, A.,
634 Kerminen, V. M., and Worsnop, D. R.: Direct Observations of Atmospheric Aerosol Nucleation,
635 Science, 339, 943-946, 10.1126/science.1227385, 2013.
636 Kupiainen-Määttä, O., Olenius, T., Korhonen, H., Malila, J., Dal Maso, M., Lehtinen, K., and Vehkamäki,
637 H.: Critical cluster size cannot in practice be determined by slope analysis in atmospherically
638 relevant applications, Journal of Aerosol Science, 77, 127-144, doi:10.1016/j.jaerosci.2014.07.005,
639 2014.
640 Kurtén, T., Noppel, M., Vehkamaeki, H., Salonen, M., and Kulmala, M.: Quantum chemical studies of
641 hydrate formation of H_2SO_4 and HSO_4^-, Boreal Environment Research, 12, 431-453, 2007.
642 Laden, F., Schwartz, J., Speizer, F. E., and Dockery, D. W.: Reduction in fine particulate air pollution and
643 mortality: extended follow-up of the Harvard Six Cities study, American journal of respiratory and
644 critical care medicine, 173, 667-672, 2006.
645 Lee, S.-H., Reeves, J., Wilson, J., Hunton, D., Viggiano, A., Miller, T., Ballenthin, J., and Lait, L.: Particle
646 formation by ion nucleation in the upper troposphere and lower stratosphere, Science, 301, 1886-
647 1889, 2003.
648 Lehtinen, K., and Kulmala, M.: A model for particle formation and growth in the atmosphere with
649 molecular resolution in size, Atmospheric Chemistry and Physics, 3, 251-257, 2003.
650 Ma, Y., Xu, X., Song, W., Geng, F., and Wang, L.: Seasonal and diurnal variations of particulate
651 organosulfates in urban Shanghai, China, Atmospheric Environment, 85, 152-160, 2014.
652 Matsui, H., Koike, M., Kondo, Y., Takegawa, N., Wiedensohler, A., Fast, J. D., and Zaveri, R. A.: Impact of
653 new particle formation on the concentrations of aerosols and cloud condensation nuclei around
654 Beijing, Journal of Geophysical Research: Atmospheres, 116, D19208, doi: 10.1029/2011JD016025,
655 2011.
656 McMurry, P. H., Fink, M., Sakurai, H., Stolzenburg, M., Mauldin, R., Smith, J., Eisele, F., Moore, K.,
657 Sjostedt, S., and Tanner, D.: A criterion for new particle formation in the sulfur-rich Atlanta
658 atmosphere, Journal of Geophysical Research: Atmospheres, 110, D22S02, doi:
659 10.1029/2005JD005901, 2005.
660 Mikkonen, S., Romakkaniemi, S., Smith, J. N., Korhonen, H., Petäjä, T., Plass-Duelmer, C., Boy, M.,
661 McMurry, P. H., Lehtinen, K. E. J., Joutsensaari, J., Hamed, A., Mauldin Iii, R. L., Birmili, W., Spindler,
662 G., Arnold, F., Kulmala, M., and Laaksonen, A.: A statistical proxy for sulphuric acid concentration,
663 Atmospheric Chemistry and Physics, 11, 11319-11334, 10.5194/acp-11-11319-2011, 2011.
664 Napari, I., Noppel, M., Vehkamäki, H., and Kulmala, M.: Parametrization of ternary nucleation rates for
665 H_2SO_4-NH_3-H_2O vapors, Journal of Geophysical Research: Atmospheres (1984–2012), 107, AAC 6-1-
666 AAC 6-6, 2002.
667 Nieminen, T., Lehtinen, K. E. J., and Kulmala, M.: Sub-10 nm particle growth by vapor condensation –
668 effects of vapor molecule size and particle thermal speed, Atmospheric Chemistry and Physics, 10,
669 9773-9779, 10.5194/acp-10-9773-2010, 2010.
670 O'Dowd, C. D., Jimenez, J. L., Bahreini, R., Flagan, R. C., Seinfeld, J. H., Hämeri, K., Pirjola, L., Kulmala,

M., Jennings, S. G., and Hoffmann, T.: Marine aerosol formation from biogenic iodine emissions, Nature, 417, 632-636, 2002.

Park, J., Sakurai, H., Vollmers, K., and McMurry, P. H.: Aerosol size distributions measured at the South Pole during ISCAT, Atmospheric Environment, 38, 5493-5500, 2004.

Platt, U., and Stutz, J.: Differential Optical Absorption Spectroscopy-Principles and Applications, Springer Berlin Heidelberg, 2008.

Pope, C. A., and Dockery, D. W.: Health effects of fine particulate air pollution: lines that connect, Journal of the Air & Waste Management Association, 56, 709-742, 2006.

Riccobono, F., Schobesberger, S., Scott, C. E., Dommen, J., Ortega, I. K., Rondo, L., Almeida, J., Amorim, A., Bianchi, F., and Breitenlechner, M.: Oxidation Products of Biogenic Emissions Contribute to Nucleation of Atmospheric Particles, Science, 344, 717-721, 2014.

Schobesberger, S., Junninen, H., Bianchi, F., Lönn, G., Ehn, M., Lehtipalo, K., Dommen, J., Ehrhart, S., Ortega, I. K., and Franchin, A.: Molecular understanding of atmospheric particle formation from sulfuric acid and large oxidized organic molecules, Proceedings of the National Academy of Sciences of the United States of America, 110, 17223-17228, 2013.

Sihto, S.-L., Kulmala, M., Kerminen, V.-M., Maso, M. D., Petäjä, T., Riipinen, I., Korhonen, H., Arnold, F., Janson, R., and Boy, M.: Atmospheric sulphuric acid and aerosol formation: implications from atmospheric measurements for nucleation and early growth mechanisms, Atmospheric Chemistry and Physics, 6, 4079-4091, 2006.

Sipila, M., Berndt, T., Petaja, T., Brus, D., Vanhanen, J., Stratmann, F., Patokoski, J., Mauldin, R. L., Hyvarinen, A. P., Lihavainen, H., and Kulmala, M.: The Role of Sulfuric Acid in Atmospheric Nucleation, Science, 327, 1243-1246, 10.1126/science.1180315, 2010.

Stolzenburg, M. R., McMurry, P. H., Sakurai, H., Smith, J. N., Mauldin, R. L., Eisele, F. L., and Clement, C. F.: Growth rates of freshly nucleated atmospheric particles in Atlanta, Journal of Geophysical Research, 110, 10.1029/2005jd005935, 2005.

Vanhanen, J., Mikkilä, J., Lehtipalo, K., Sipilä, M., Manninen, H., Siivola, E., Petäjä, T., and Kulmala, M.: Particle size magnifier for nano-CN detection, Aerosol Science and Technology, 45, 533-542, 2011.

Wang, L., Khalizov, A. F., Zheng, J., Xu, W., Ma, Y., Lal, V., and Zhang, R.: Atmospheric nanoparticles formed from heterogeneous reactions of organics, Nature Geoscience, 3, 238-242, 2010.

Wang, L., Xu, W., Khalizov, A. F., Zheng, J., Qiu, C., and Zhang, R.: Laboratory investigation on the role of organics in atmospheric nanoparticle growth, The Journal of Physical Chemistry A, 115, 8940-8947, 2011.

Wang, L., Du, H., Chen, J., Zhang, M., Huang, X., Tan, H., Kong, L., and Geng, F.: Consecutive transport of anthropogenic air masses and dust storm plume: Two case events at Shanghai, China, Atmospheric Research, 127, 22-33, 2013.

Wang, S., Zhou, R., Zhao, H., Wang, Z., Chen, L., and Zhou, B.: Long-term observation of atmospheric nitrous acid (HONO) and its implication to local NO_2 levels in Shanghai, China, Atmospheric Environment, 77, 718-724, 10.1016/j.atmosenv.2013.05.071, 2013.

Weber, R., Marti, J., McMurry, P., Eisele, F., Tanner, D., and Jefferson, A.: Measured atmospheric new particle formation rates: Implications for nucleation mechanisms, Chemical Engineering Communications, 151, 53-64, 1996.

Wu, Z., Hu, M., Liu, S., Wehner, B., Bauer, S., Ma ßling, A., Wiedensohler, A., Petäjä, T., Dal Maso, M., and Kulmala, M.: New particle formation in Beijing, China: Statistical analysis of a 1-year data set, Journal of Geophysical Research-Atmospheres, 112, D09209, doi:10.1029/2006jd007406, 2007.

Yu, F., and Turco, R. P.: From molecular clusters to nanoparticles: Role of ambient ionization in tropospheric aerosol formation, Journal of Geophysical Research: Atmospheres (1984–2012), 106, 4797-4814, 2001.

Yu, F. Q., and Hallar, A. G.: Difference in particle formation at a mountaintop location during spring and summer: Implications for the role of sulfuric acid and organics in nucleation, Journal of Geophysical Research-Atmospheres, 119, 12246-12255, 2014.

Yu, H., Gannet Hallar, A., You, Y., Sedlacek, A., Springston, S., Kanawade, V. P., Lee, Y. N., Wang, J., Kuang, C., and McGraw, R. L.: Sub-3 nm particles observed at the coastal and continental sites in the United States, Journal of Geophysical Research: Atmospheres, 119, 860-879, doi: 10.1002/2013JD020841, 2014.

Yue, D., Hu, M., Wu, Z., Wang, Z., Guo, S., Wehner, B., Nowak, A., Achtert, P., Wiedensohler, A., Jung, J., Kim, Y. J., and Liu, S.: Characteristics of aerosol size distributions and new particle formation in the summer in Beijing, Journal of Geophysical Research, 114, D00G12, doi:10.1029/2008jd010894, 2009.

Yue, D. L., Hu, M., Zhang, R. Y., Wang, Z. B., Zheng, J., Wu, Z. J., Wiedensohler, A., He, L. Y., Huang, X. F., and Zhu, T.: The roles of sulfuric acid in new particle formation and growth in the mega-city of Beijing, Atmospheric Chemistry and Physics, 10, 4953-4960, 10.5194/acp-10-4953-2010, 2010.

Yue, D. L., Hu, M., Zhang, R. Y., Wu, Z. J., Su, H., Wang, Z. B., Peng, J. F., He, L. Y., Huang, X. F., Gong, Y. G., and Wiedensohler, A.: Potential contribution of new particle formation to cloud condensation nuclei in Beijing, Atmospheric Environment, 45, 6070-6077, 10.1016/j.atmosenv.2011.07.037, 2011.

Yue, D. L., Hu, M., Wang, Z. B., Wen, M. T., Guo, S., Zhong, L. J., Wiedensohler, A., and Zhang, Y. H.: Comparison of particle number size distributions and new particle formation between the urban and rural sites in the PRD region, China, Atmospheric Environment, 76, 181-188, 10.1016/j.atmosenv.2012.11.018, 2013.

Zhang, R., Suh, I., Zhao, J., Zhang, D., Fortner, E. C., Tie, X., Molina, L. T., and Molina, M. J.: Atmospheric new particle formation enhanced by organic acids, Science, 304, 1487-1490, 2004.

Zhang, R., Wang, L., Khalizov, A. F., Zhao, J., Zheng, J., McGraw, R. L., and Molina, L. T.: Formation of nanoparticles of blue haze enhanced by anthropogenic pollution, Proceedings of the National Academy of Sciences of the United States of America, 106, 17650-17654, 2009.

Zhang, R., Khalizov, A., Wang, L., Hu, M., and Xu, W.: Nucleation and Growth of Nanoparticles in the Atmosphere, Chemical Reviews, 112, 1957-2011, 10.1021/cr2001756, 2012.

Zhang, Y., Zhang, X., Sun, J., Lin, W., Gong, S., Shen, X., and Yang, S.: Characterization of new particle and secondary aerosol formation during summertime in Beijing, China, Tellus B, 63, 382-394, 2011.

Zhao, J., Smith, J., Eisele, F., Chen, M., Kuang, C., and McMurry, P.: Observation of neutral sulfuric acid-amine containing clusters in laboratory and ambient measurements, Atmospheric Chemistry and Physics, 11, 10823-10836, 2011.

Zheng, J., Hu, M., Zhang, R., Yue, D., Wang, Z., Guo, S., Li, X., Bohn, B., Shao, M., and He, L.: Measurements of gaseous H_2SO_4 by AP-ID-CIMS during CAREBeijing 2008 campaign, Atmospheric Chemistry and Physics, 11, 7755-7765, 2011.

Zheng, J., Ma, Y., Chen, M., Zhang, Q., Wang, L., Khalizov, A. F., Yao, L., Wang, Z., Wang, X., and Chen, L.: Measurement of atmospheric amines and ammonia using the high resolution time-of-flight chemical ionization mass spectrometry, Atmospheric Environment, 102, 249-259, 10.1016/j.atmosenv.2014.12.002, 2015.

759

760

Table 1. Nucleation rate ($J_{1.34}$), formation rate of 3 nm particles (J_3), particle growth rates ($GR_{1.35\sim2.39}$, $GR_{2.39\sim7}$, and $GR_{7\sim20}$), condensation sink (CS), sulfuric acid proxy ($[H_2SO_4]$), number concentrations of 1.34-3 nm clusters/particles($N_{1.34\sim3}$), and total number concentrations of particles $N_{1.34\sim615}$, of each NPF event during this campaign

Date	$J_{1.34}$ ($cm^{-3}\ s^{-1}$)	J_3 ($cm^{-3}\ s^{-1}$)	$GR_{1.35\sim2.39}$ (nm h^{-1})	$GR_{2.39\sim7}$ (nm h^{-1})	$GR_{7\sim20}$ (nm h^{-1})	CS [e] ($10^{-2}\ s^{-1}$)	$[H_2SO_4]$ [e] ($10^7\ cm^{-3}$)	$N_{1.34\sim3}$ [f] ($10^4\ cm^{-3}$)	$N_{1.34\sim615}$ [f] ($10^4\ cm^{-3}$)	Ref.
Nov. 25th, 2013	n.a.[a]	10.6	n.a.	12.4[b]	38.3	4.7	2.7	3.3[g]	6.3	this study
Nov. 26th, 2013	n.a.	2.3	n.a.	0.32[b]	n.a.	5.9	2.6	n.a.	n.a.	this study
Nov. 28th, 2013	185.1	13.4	0.94	35.7	4.6	5.7	3.6	1.6	4.2	this study
Nov. 29th, 2013	271.0	3.9	1.7	10.6	4.5	6.3	4.3	2.1	4.5	this study
Nov. 30th, 2013	n.a	n.a.	0.82	3.4	10.2	n.a.	3.1	1.5	n.a.	this study
Dec. 10th, 2013	268.4	10.0	0.49	18.6	21.0	9.9	5.5	1.4	4.6	this study
Dec. 11th, 2013	219.0	19.2	n.a.	5.1	9.6	10.2	6.4	1.1	4.5	this study
Dec. 12th, 2013	190.3	7.6	n.a.	3.1	12.3	8.8	4.5	1.1	4.1	this study
Jan. 9th, 2014	136.2	n.a.	8.1	n.a.	9.5	3.7	2.3	1.6	3.8	this study
Jan. 13th, 2014	n.a.	2.7	n.a.	6.3	1.9	3.0	2.3	1.5	3.4	this study
Jan. 15th, 2014	121.9	n.a.	0.56	n.a.	9.7	4.2	4.1	1.5	4.3	this study
Jan. 21st, 2014	112.4	9.2	1.5	11.9	7.5	4.9	3.7	1.1	3.9	this study
Jan. 24th, 2014	n.a.	8.1	n.a.	12.2[b]	7.8	4.7	3.4	1.7	4.2	this study
Mean	**188.0**	**8.7**	**2.0**	**10.9**	**11.4**	**6.0**	**3.7**	**1.5**	**4.4**	this study
Finland	1.4	0.61	1.4	3.9	4.9	0.05-0.35				Kulmala et al. (2012)
USA[h]	1.3					0.8		0.9		Yu et al. (2014)
Atlanta					3-20[c]					Stolzenburg et al. (2005)
Atlanta			5.5-7.6							Kuang et al. (2012)
Beijing					1.2-8.0[c]	2.4-3.6				Gao et al. (2012)
Beijing		3.3-81.4			0.1-11.2[c]	0.58-4.3				Wu et al. (2007)
Beijing					2.7-13.9[c]	0.6-8.4				Zhang et al. (2011)
Beijing		1.1-22.4			1.2-5.6[c]	0.9-5.3				Yue et al. (2009)
Nanjing	33.2[i]	1.1[j]		6.3	8[d]	2.4				Herrmann et al. (2014)
Hong Kong		3.6-6.9			1.5-8.4[c]	1.0-6.2				Guo et al. (2012)
Pearl River Delta		2.4-4.0(rural)			4.0-22.7(rural) 10.1-18.9(urban)	2.3-3.3(rural) 3.5-4.6(urban)				Yue et al. (2013)

[a] Data were not available or could not be accurately determined; [b] Result were calculated from nano-SMPS data; [c] Shown here is $GR_{3\sim30}$; [d] Shown here is $GR_{7\sim30}$; [e] Daytime average (from 6:00 am to 6:00 pm); [f] 24hr-average; [g] Average values between 10 am and 4 pm; [h] Shown here are data in Kent, OH; [i] Shown here is J_2 ; [j] Shown here is J_6 .

Figure Captions

Figure 1. Contour plot for particle size distributions of 3-615 nm and plot of number concentrations of sub-3 nm clusters/particles ($N_{1.34\text{-}3}$) during Nov. 25th, 2013 - Jan. 25th, 2014. Data were occasionally missing because of the maintenance and minor breakdown of instruments. NPF events are illustrated with shadows.

Figure 2. Profiles of $N_{1.34\text{-}3}$, $N_{3\text{~}7}$, and $N_{7\text{~}30}$ from 6 am to 6 pm on a NPF day (Dec. 11th, 2013) and a non-NPF day (Jan. 7th, 2014), respectively.

Figure 3. Averaged particle size evolution on NPF days. Arithmetic mean of particle growth rates are given with one standard deviation.

Figure 4. Correlation between $\log J_{1.34}$ and $\log[H_2SO_4]$. Daily peak concentration of sulfuric acid proxy was used as an approximation for its effective concentration on a NPF day. The error bar corresponds to a 42% uncertainty of sulfuric acid proxy according to Mikkonen et al., (2011).

Figure 5. Correlation between $\log J_{1.34}$ and $\log[NH_3]$. Daytime average of ammonia was used as an approximation for its effective concentration on a NPF day. The error bar represents the standard deviation of the daytime average concentration of ammonia.

Figure 6. Relative contribution of sulfuric acid to growth of particles in the range of 3-7 and 7-20 nm, respectively, on each NPF day.

Figure 7. Number concentrations of 1.34-10 nm particles ($N_{1.34\text{~}10}$), sulfuric acid proxy ($[H_2SO_4]$), concentrations of ammonia, and aerosol surface area during the campaign. NPF events are illustrated with shadows.

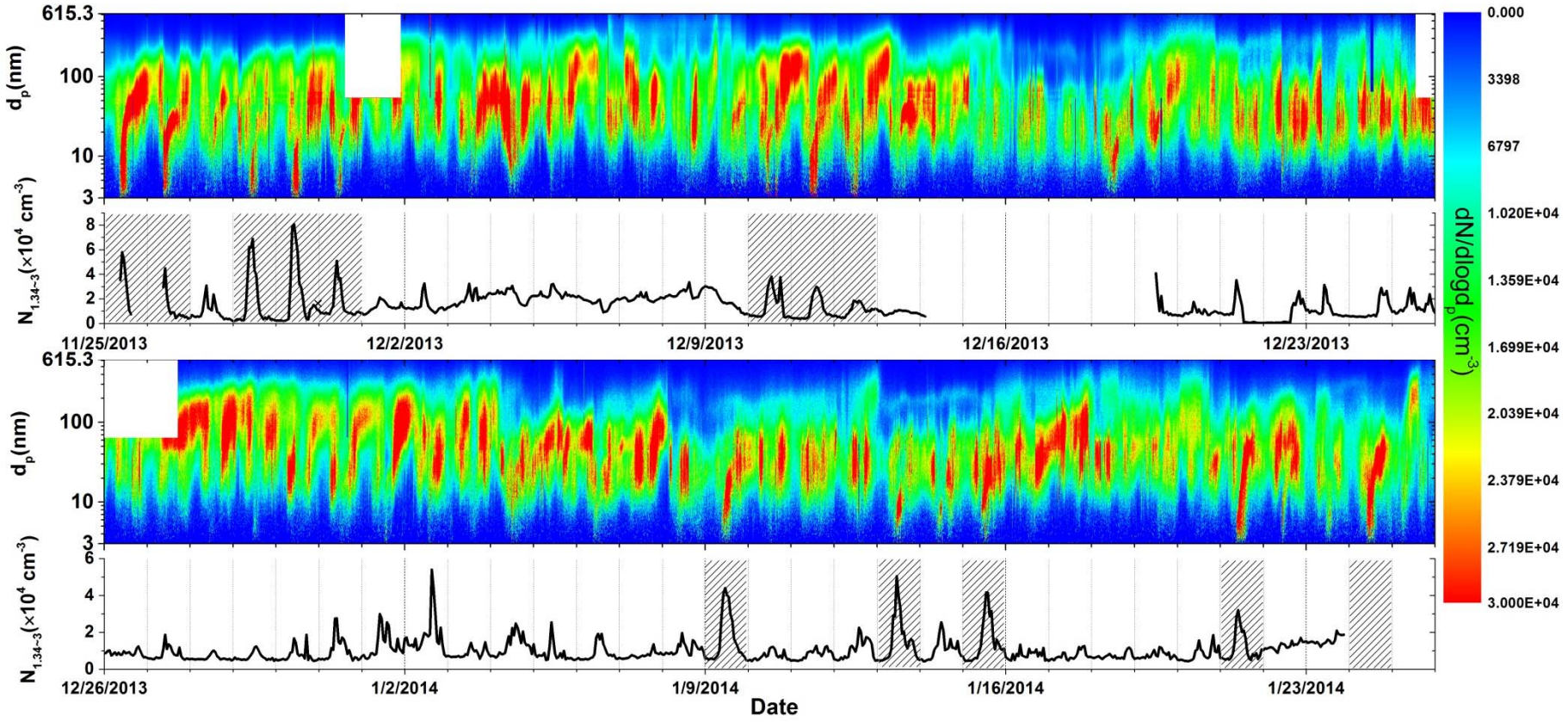
615.3
100
10
3
d_p(nm)
$N_{1.34-3}$($\times10^4$ cm^{-3})
11/25/2013
12/2/2013
12/9/2013
12/16/2013
12/23/2013
12/26/2013
1/2/2014
1/9/2014
1/16/2014
1/23/2014
Date
dN/dlogd_p(cm^{-3})
0.000
3398
6797
1.020E+04
1.359E+04
1.699E+04
2.039E+04
2.379E+04
2.719E+04
3.000E+04

Figure 1.

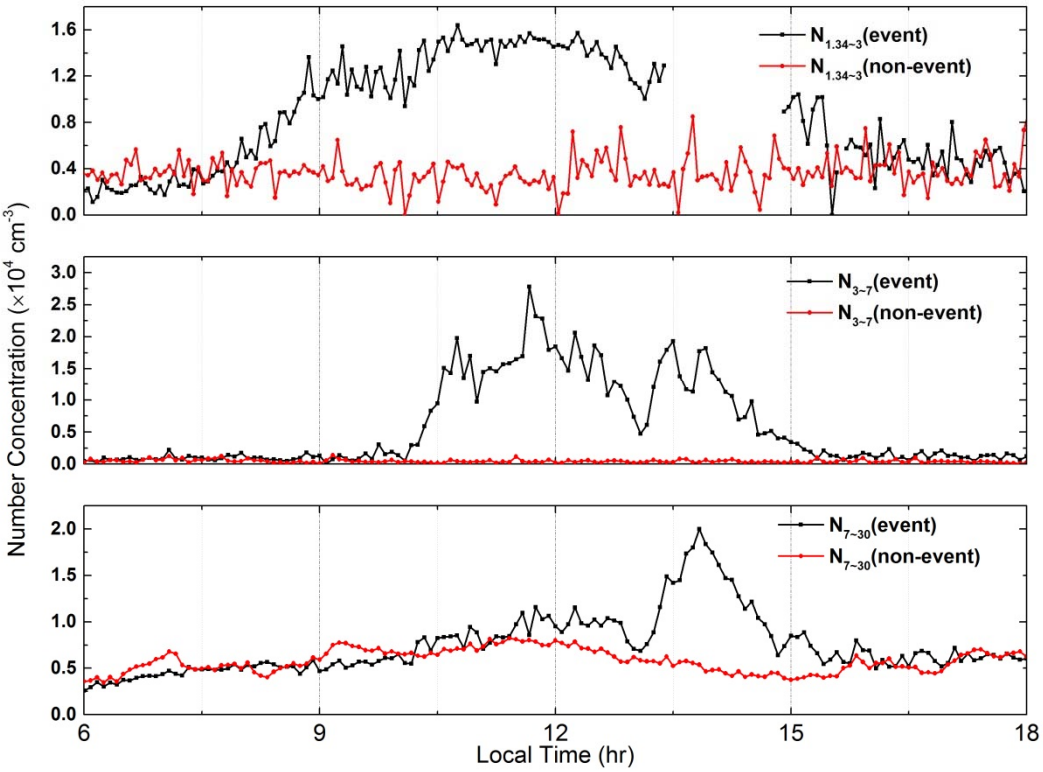
N1.34~3(event)
N1.34~3(non-event)
N3~7(event)
N3~7(non-event)
N7~30(event)
N7~30(non-event)
Number Concentration (×10^4 cm^-3)
Local Time (hr)
0.0
0.4
0.8
1.2
1.6
0.5
1.0
1.5
2.0
2.5
3.0
6
9
12
15
18

Figure 2.

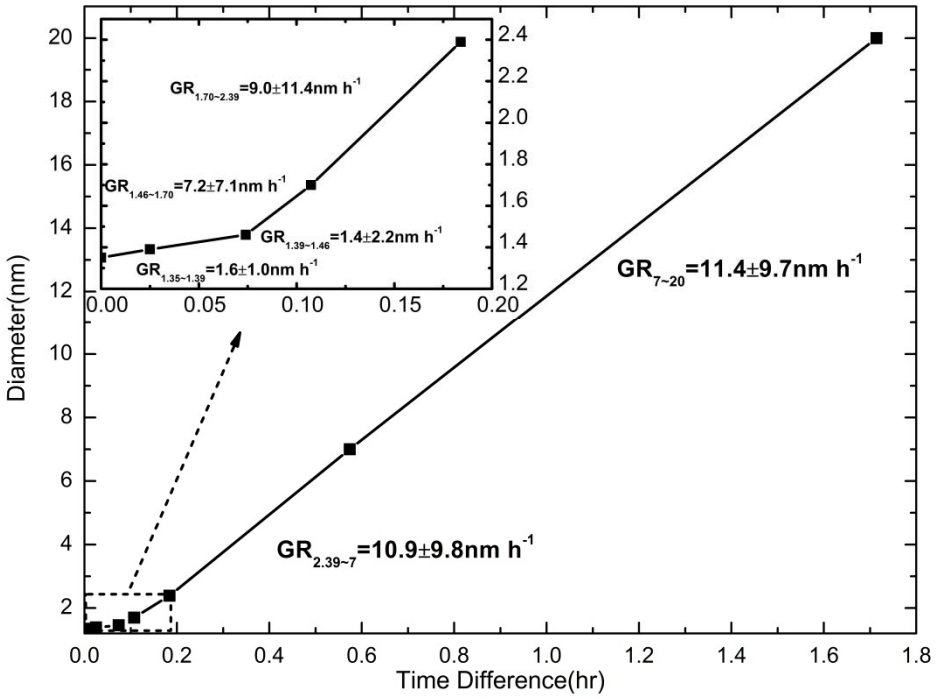

Figure 3.

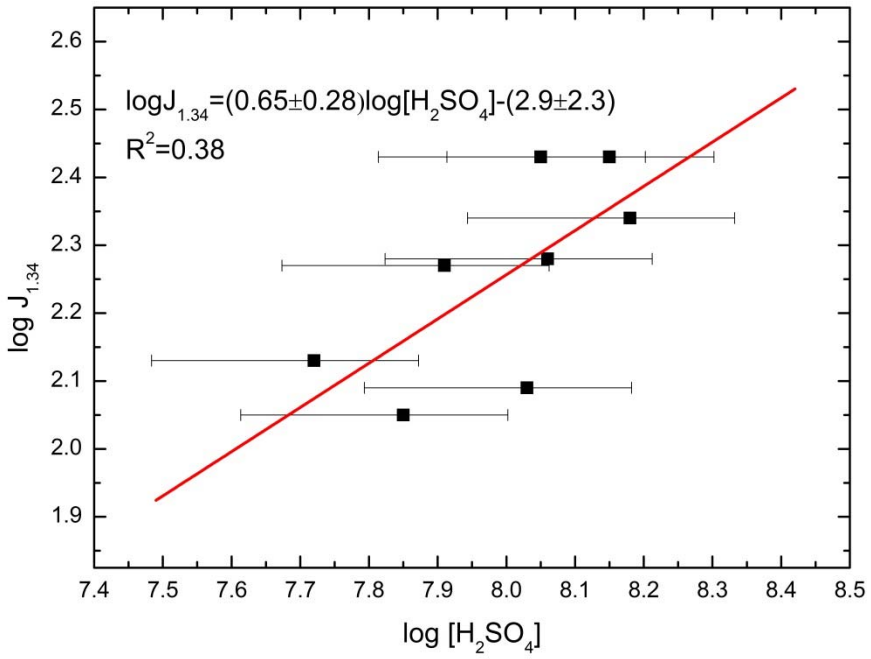

Figure 4.

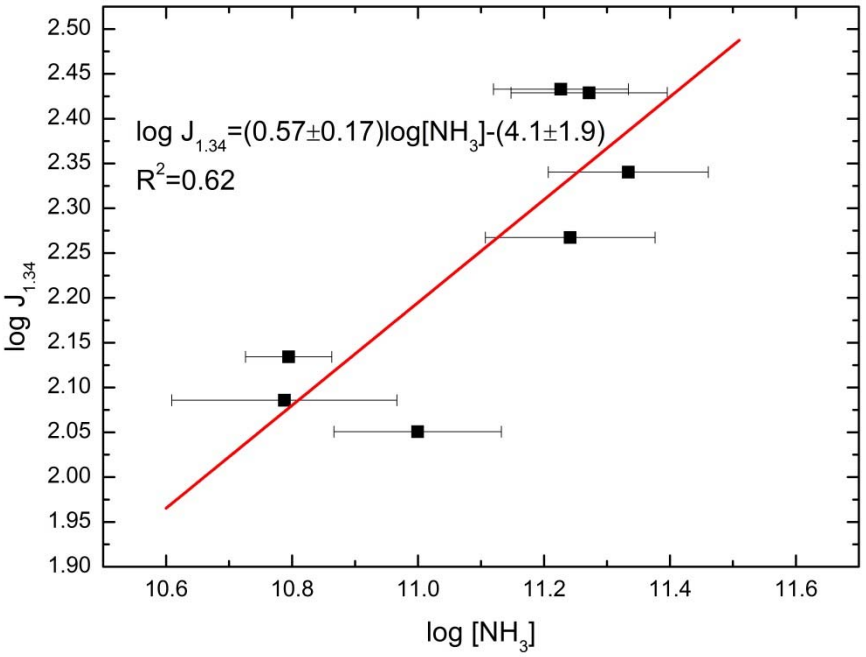

Figure 5.

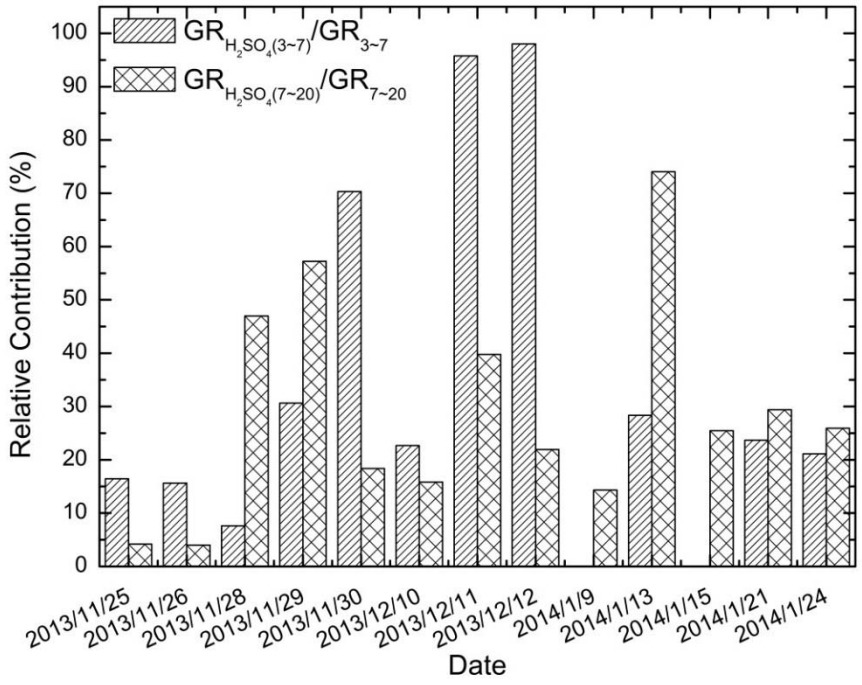

Figure 6.

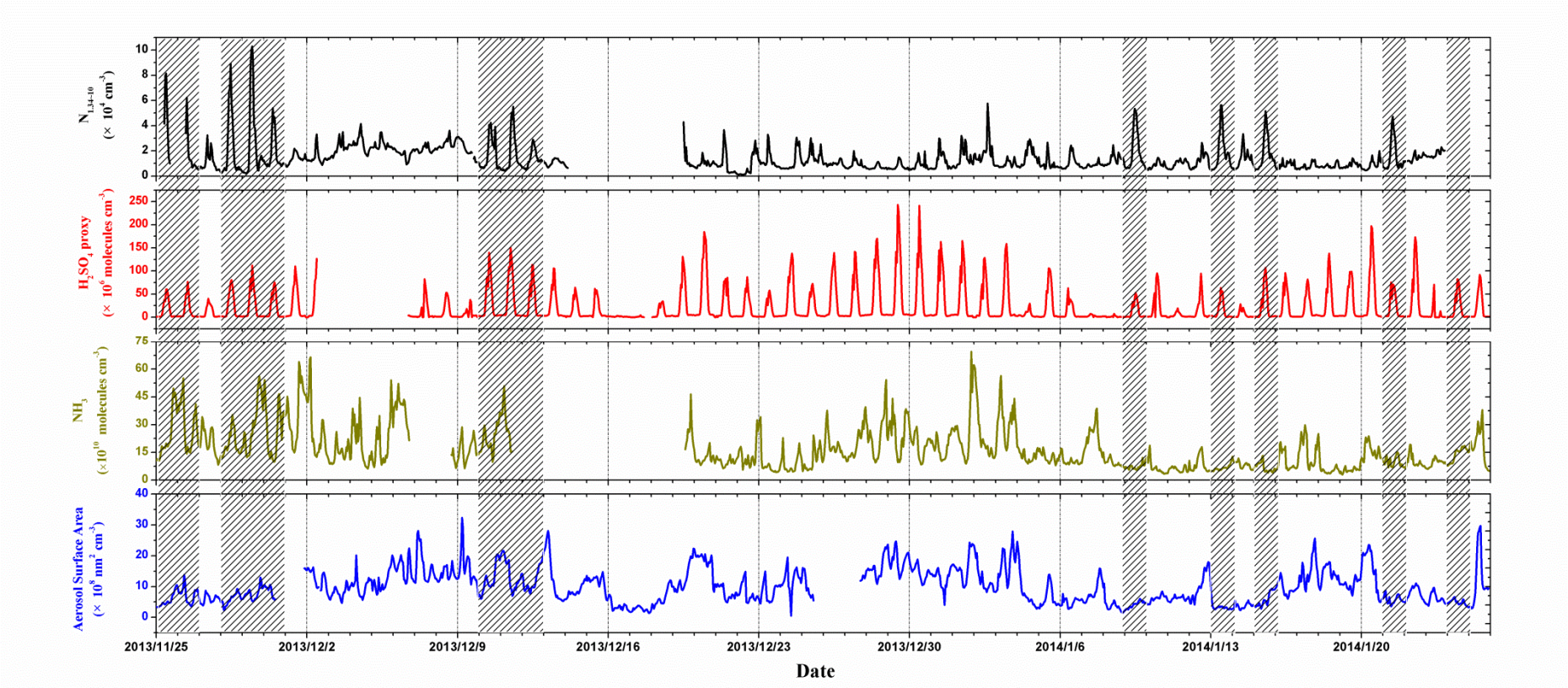
$N_{1.34-10}$ (× 10^4 cm^{-3})
H_2SO_4 proxy (× 10^6 molecules cm^{-3})
NH_3 (×10^{10} molecules cm^{-3})
Aerosol Surface Area (× 10^9 nm^2 cm^{-3})
2013/11/25
2013/12/2
2013/12/9
2013/12/16
2013/12/23
2013/12/30
2014/1/6
2014/1/13
2014/1/20
Date

Figure 7